AMERICAN SOCIETY FOR MICROBIOLOGY | Applied and Environmental Microbiology®

GENETICS AND MOLECULAR BIOLOGY

Functional Analysis of Phenazine Biosynthesis Genes in *Burkholderia* spp.

Samuel Hendry,[a] Stephan Steinke,[b] Kathrin Wittstein,[c] Marc Stadler,[d,e] Kirsten Harmrolfs,[f] Yetunde Adewunmi,[a] Gyan Sahukhal,[a] Mohamed Elasri,[a] Linda Thomashow,[g] David Weller,[g] Olga Mavrodi,[a] Wulf Blankenfeldt,[b,c] Dmitri Mavrodi[a]

[a]Center for Molecular and Cellular Biosciences, School of Biological, Environmental, and Earth Sciences, University of Southern Mississippi, Hattiesburg, Mississippi, USA
[b]Structure and Function of Proteins, Helmholtz Centre for Infection Research, Braunschweig, Germany
[c]Institute for Biochemistry, Biotechnology and Bioinformatics, Technische Universität Braunschweig, Braunschweig, Germany
[d]Microbial Drugs, Helmholtz Centre for Infection Research, Braunschweig, Germany
[e]Institute of Microbiology, Technische Universität Braunschweig, Braunschweig, Germany
[f]Chemical Biology, Helmholtz Centre for Infection Research, Braunschweig, Germany
[g]Wheat Health, Genetics and Quality Research Unit, USDA Agricultural Research Service, Pullman, Washington, USA

Samuel Hendry, Stephan Steinke, and Kathrin Wittstein contributed equally to this study. The order of names was determined based on alphabetical order.

ABSTRACT *Burkholderia* encompasses a group of ubiquitous Gram-negative bacteria that includes numerous saprophytes as well as species that cause infections in animals, immunocompromised patients, and plants. Some species of *Burkholderia* produce colored, redox-active secondary metabolites called phenazines. Phenazines contribute to competitiveness, biofilm formation, and virulence in the opportunistic pathogen *Pseudomonas aeruginosa*, but knowledge of their diversity, biosynthesis, and biological functions in *Burkholderia* is lacking. In this study, we screened publicly accessible genome sequence databases and identified phenazine biosynthesis genes in multiple strains of the *Burkholderia cepacia* complex, some isolates of the *B. pseudomallei* clade, and the plant pathogen *B. glumae*. We then focused on *B. lata* ATCC 17760 to reveal the organization and function of genes involved in the production of dimethyl 4,9-dihydroxy-1,6-phenazinedicarboxylate. Using a combination of isogenic mutants and plasmids carrying different segments of the *phz* locus, we characterized three novel genes involved in the modification of the phenazine tricycle. Our functional studies revealed a connection between the presence and amount of phenazines and the dynamics of biofilm growth in flow cell and static experimental systems but at the same time failed to link the production of phenazines with the capacity of *Burkholderia* to kill fruit flies and rot onions.

IMPORTANCE Although the production of phenazines in *Burkholderia* was first reported almost 70 years ago, the role these metabolites play in the biology of these economically important microorganisms remains poorly understood. Our results revealed that the phenazine biosynthetic pathway in *Burkholderia* has a complex evolutionary history, which likely involved horizontal gene transfers among several distantly related groups of organisms. The contribution of phenazines to the formation of biofilms suggests that *Burkholderia*, like fluorescent pseudomonads, may benefit from the unique redox-cycling properties of these versatile secondary metabolites.

KEYWORDS phenazine, biosynthesis, *Burkholderia*

Burkholderia comprises a ubiquitous group of Gram-negative bacteria that includes numerous saprophytes as well as species associated with infectious diseases, hospital-acquired infections, and necrotizing pneumonia in individuals with cystic fibrosis (1). These organisms were previously classified as *Pseudomonas*, but the advent of

Citation Hendry S, Steinke S, Wittstein K, Stadler M, Harmrolfs K, Adewunmi Y, Sahukhal G, Elasri M, Thomashow L, Weller D, Mavrodi O, Blankenfeldt W, Mavrodi D. 2021. Functional analysis of phenazine biosynthesis genes in *Burkholderia* spp. Appl Environ Microbiol 87:e02348-20. https://doi.org/10.1128/AEM.02348-20.

Editor Rebecca E. Parales, University of California, Davis

Address correspondence to Wulf Blankenfeldt, Wulf.Blankenfeldt@helmholtz-hzi.de, or Dmitri Mavrodi, dmitri.mavrodi@usm.edu.

Received 22 September 2020
Accepted 9 March 2021
Accepted manuscript posted online 19 March 2021
Published 11 May 2021

molecular and genetic techniques ultimately identified *Burkholderia* species as members of a distinct genus within *Betaproteobacteria* (2–4). Their taxonomic status was revised further in 2014 by dividing the group into two genera, with *Burkholderia* containing opportunistic pathogens of animal and plants and a new genus, *Paraburkholderia*, harboring environmental species and nitrogen-fixing mutualists (5). Subsequent studies established the polyphyletic nature of the *Burkholderia* and *Paraburkholderia* groups and separated several species into another genus, *Caballeronia* (6).

The genus *Burkholderia* encompasses over 100 species comprising three distinct lineages of *Burkholderia sensu stricto*: (i) the *Burkholderia pseudomallei* clade of mammalian pathogens, (ii) the *Burkholderia cepacia* complex (Bcc) of opportunistic pathogens, and (iii) the *B. glumae*/*B. gladioli* clade of plant pathogens (5). The *B. pseudomallei* clade includes closely related infectious agents associated with serious infections in humans and animals (7, 8). *B. pseudomallei*, a common soil and freshwater saprophyte, causes melioidosis, a condition associated with nearly 20% of cases of acquired septicemia in Southeast Asia and Northern Australia (9). Unlike *B. pseudomallei*, *B. mallei* is an obligate mammalian pathogen with a smaller multireplicon genome. Although primarily a pathogen of equines, in which it causes glanders, *B. mallei* is also capable of infecting humans through contact with diseased animals (10).

The *Burkholderia cepacia* complex (Bcc) is named after the type species of the genus and includes microorganisms that are common in the environment, though under favorable conditions they can act as opportunistic human pathogens (11). Many *Burkholderia* spp. are typical saprophytes and are particularly abundant in areas with acidic soils (12), while others colonize eukaryotic hosts and include both commensals and economically important pathogens of plants and animals. Species of the Bcc complex catabolize a wide variety of organic compounds as energy sources, produce an impressive array of secondary metabolites, and provide plant-growth-promoting and biocontrol properties (3). However, many members of the Bcc group have emerged as causal agents of severe nosocomial infections in immunocompromised patients and individuals with cystic fibrosis (11, 13). Strains of the *B. cepacia* complex also are intrinsically resistant to a wide range of antibiotics, form robust biofilms, and have multiple mechanisms to resist oxidative stress and sequester iron, making infections particularly challenging to treat (14, 15).

Finally, species of the *B. glumae*/*B. gladioli* clade colonize plant tissues externally or endophytically (16) and maintain commensal or pathogenic relationships with their hosts. For example, *B. gladioli* pv. *allicola* causes slippery skin of onions, during which the pathogen affects both the aboveground parts of the plant and the bulbs (17). Other pathovars of *B. gladioli* damage bulbs of gladioli and irises and infect certain species of orchids (18), while *B. gladioli* pv. *agaricicola* produces a variety of antifungal secondary metabolites and is an important pathogen in the mushroom industry (19). Another serious phytopathogen in this group is *B. glumae*, which is associated with bacterial blight of rice. Although *B. glumae* and *B. gladioli* are typically considered plant pathogens, strains of both species have been isolated from immunocompromised individuals or patients with cystic fibrosis, highlighting the remarkable versatility of these organisms and their capacity to adapt and thrive in diverse environments (20, 21).

Some strains of *Burkholderia* produce the colored, redox-active secondary metabolites of the phenazine group (22, 23). Microbial phenazines are structurally diverse, but all share a conserved nitrogen-containing tricyclic core assembled by products of a conserved seven-gene operon, *phzABCDEFG*, termed the "core phenazine biosynthesis genes" (24). The expression of the core genes in *Pseudomonas* yields phenazine-1-carboxylic acid (PCA), whereas the final product synthesized by other groups of bacteria is phenazine-1,6-dicarboxylic acid (PDC). In addition to the highly conserved core genes, many producers carry extensive sets of auxiliary genes that encode enzymes responsible for converting PCA and PDC into species-specific phenazine metabolites, as well as proteins that perform efflux, resistance, and regulatory functions (25–27).

Natural phenazines are now known to play an important role in the biology of the

strains that produce them. Phenazines are electron shuttles that reduce molecular oxygen and generate toxic reactive oxygen species, making these metabolites broadly inhibitory to bacteria, fungi, and parasites (23). Structurally simple phenazines produced by beneficial strains of the *Pseudomonas fluorescens* complex and *Pantoea agglomerans* suppress pathogens that cause plant diseases (28, 29). Pyocyanin synthesized by *Pseudomonas aeruginosa* is critical for lung infection in mice (30) and has been detected at concentrations up to 10^{-4} M in the sputa of patients with cystic fibrosis (31). This metabolite acts as a host-nonspecific pathogenicity factor enabling the producing strains to kill *Drosophila melanogaster* and *Caenorhabditis elegans* (32–34). Phenazines also function as signals that control gene expression and colony morphogenesis in bacteria (35, 36), while phenazine-1-carboxamide protects *P. aeruginosa* from predation by triggering avoidance behavior in bacterivorous nematodes (37). Finally, by acting as electron shuttles, phenazines help aerobic bacteria maintain redox homeostasis in low-oxygen environments by passing electrons from intracellular NADH to oxidized extracellular phenazine (38). The ability to mediate the reoxidation of NADH under oxygen-limiting conditions explains the importance of phenazine production for biofilm formation, as mature biofilms are often hypoxic (35).

The production of phenazines in *Burkholderia* was first reported in the 1950s, when several studies reported their isolation from *Pseudomonas multivorans*, *Pseudomonas cepacia*, and *Pseudomonas phenazinium* (all later reclassified as *Burkholderia* and *Paraburkholderia*) (22, 39–41). Phenazines produced by *B. glumae* were described much later (42). Further testing also revealed the broad-spectrum antimicrobial properties of *Burkholderia* phenazines (23, 42, 43). The genetic basis for the production of these versatile metabolites in *Burkholderia* spp. remained unexplored until recently, when we employed a series of primers and probes targeting the core phenazine biosynthesis gene *phzF* to demonstrate the presence of *phz* genes in multiple strains of *Burkholderia* (25). Dar et al. (27) also have confirmed the presence of phenazine-producing *Burkholderiales* representatives in multiple agricultural soils and crop microbiomes. Despite this progress, the role these metabolites play in the biology of *Burkholderia* remains poorly understood. In this study, we addressed these gaps by focusing on the diversity, biosynthesis, and function of phenazines from *B. lata* ATCC 17760.

RESULTS

Screening *Burkholderia* genomes for the presence of phenazine genes. Screening of publicly accessible databases yielded numerous genome sequences of *Burkholderia* bacteria carrying phenazine biosynthesis genes. Overall, phenazine gene clusters were identified in 20 strains of *Burkholderia* and in one strain of *Paraburkholderia* that belong to different species of the two genera. According to GenBank records, most of these genomes came from strains isolated from samples of soil collected in the Northern Territory of Australia. Two more Australian strains (BDU5 and BDU6) were isolated from soil on Badu Island in the Torres Strait, and another one (TSV85) was isolated from water collected in Townsville, Queensland. Both genomes of *B. glumae* (BGR1 and LMG 2196) belonged to strains isolated from rice in Japan (44, 45), whereas *B. lata* ATCC 17760 originated from soil collected in Trinidad (46). In addition to publicly available genomes, we sequenced and annotated draft genome sequences of three *Burkholderia* strains with phenazine genes. Two of these strains, *Burkholderia* sp. 2424 and PC17, were isolated in Japan (47), whereas the third strain, *Burkholderia* sp. 5.5B, is a soil isolate and biological control agent from the United States (43). Finally, in the *Paraburkholderia* group, phenazine genes were present in just one strain, the soil isolate *Paraburkholderia phenazinium* LMG 2247 (39). Phylograms inferred from 16S rRNA sequences revealed that most *Burkholderia* species carrying phenazine gene clusters belonged to the Bcc group (see Fig. S1 in the supplemental material). Phenazine genes were also present in the plant pathogen *B. glumae* and in some strains of the *B. pseudomallei* clade. Although the phylogeny was overall robust, the high degree of

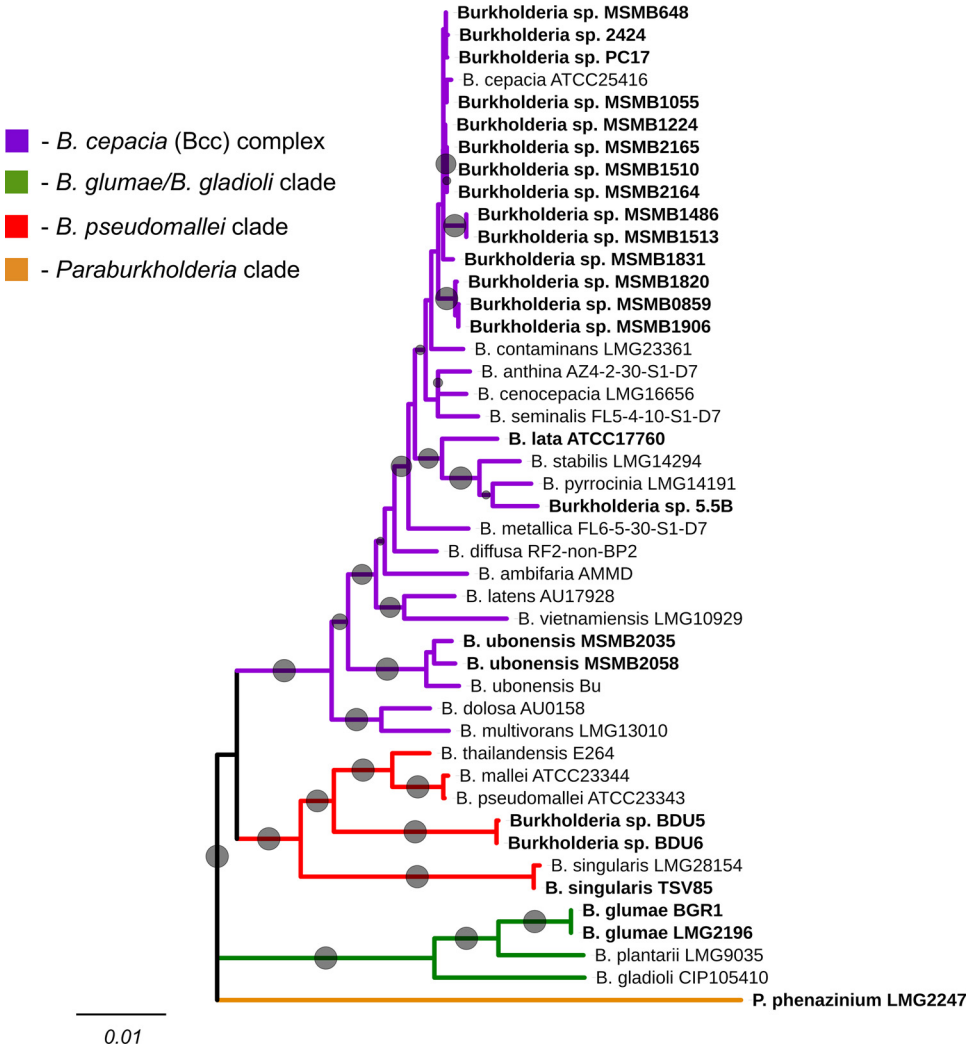

FIG 1 Multilocus sequence typing phylogeny of *Burkholderia* spp. Neighbor-joining phylogeny inferred from concatenated protein sequences (4,458 characters) of housekeeping enzymes AtpD, GltB, GyrB, RecA, LepA, PhaC, and TrpB. Sequences from *P. phenazinium* LMG 2247^T were used as an outgroup. Strains carrying phenazine biosynthesis genes are highlighted in bold font. Indels were ignored in the analysis, and evolutionary distances were estimated using the Jukes-Cantor genetic distance model. The reproducibility of clades was assessed by bootstrap resampling, and bootstrap values greater than 60% are indicated by gray circles at the nodes (circle sizes are proportional to bootstrap values). The branch lengths are proportional to the amount of evolutionary change. The scale bars indicate substitution per site. A list of orthologous protein families is provided in Table S2.

conservation of 16S rRNA sequences did not allow us to assign strains BDU5 and TSV85 to any clade of *Burkholderia* spp.

To increase the resolution of this analysis, we repeated it with seven housekeeping genes employed in multilocus sequence typing (MLST) of the Bcc group (48) (Fig. 1). The data set included concatenated amino acid sequences of the products of *atpD* (ATP synthase beta chain), *gltB* (glutamate synthase large subunit), *gyrB* (DNA gyrase subunit B), *recA* (recombinase A), *lepA* (GTP binding protein), *phaC* (acetoacetyl-CoA reductase), and *trpB* (tryptophan synthase subunit B). The resultant well-resolved phylogeny agreed with the16S rRNA gene analysis and unambiguously identified strains BDU5, BDU6, and TSV85 as members of the *B. pseudomallei* clade (Fig. 1). The MLST-based phylogeny of the Bcc clade also confirmed that most strains with phenazine genes were closely related to the primary species of the genus, *B. cepacia*, while the rest clustered with type strains of *B. lata*, *B. pyrrocinia*, and *B. ubonensis*.

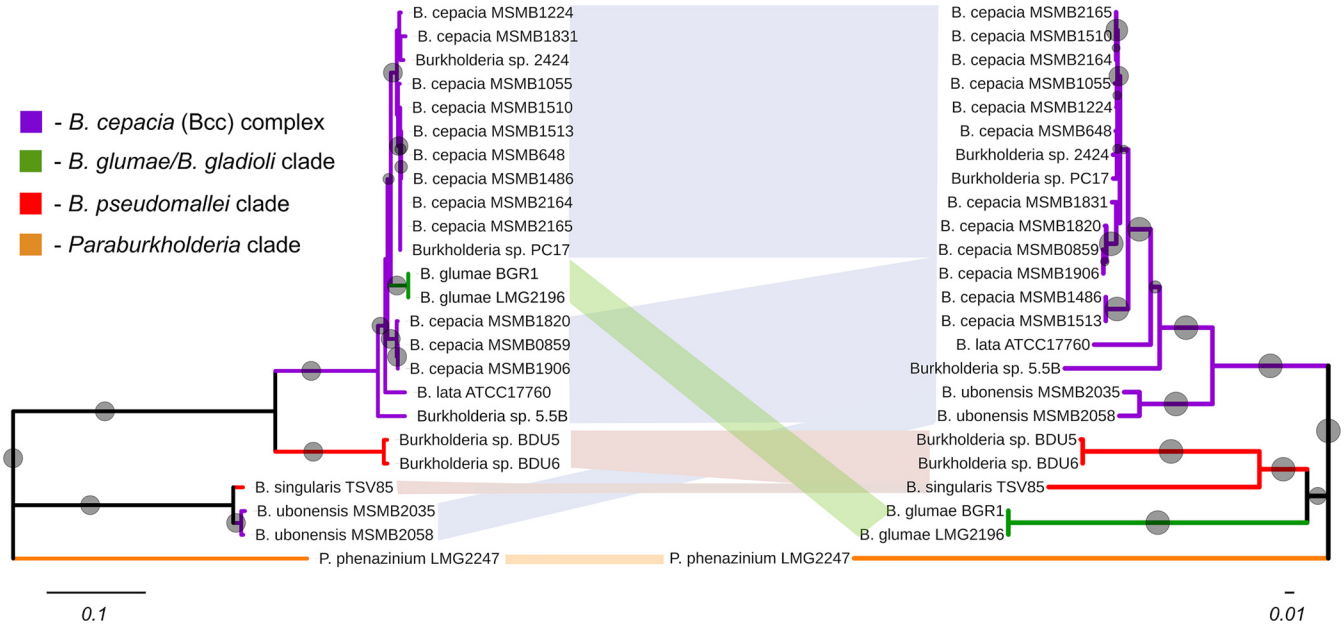

FIG 2 Contrasting phylogenies using Phz proteins and housekeeping enzymes. In some species of *Burkholderia*, phenazine genes may have been acquired via horizontal gene transfer. Contrasting neighbor-joining phylogenies inferred from concatenated sequences of PhzA/B, PhzE, and PhzG proteins (left) and housekeeping enzymes AtpD, GltB, GyrB, RecA, LepA, PhaC, and TrpB (right). Indels were ignored in the analysis, and the concatenated Phz and housekeeping data sets contained 1,024 and 4,458 characters, respectively. Sequences from *P. phenazinium* LMG 2247^T were used as an outgroup. Evolutionary distances were estimated using the Jukes-Cantor genetic distance model. The reproducibility of clades was assessed by bootstrap resampling with 1,000 pseudoreplicates, and bootstrap values greater than 60% are indicated by gray circles at the nodes (circle sizes are proportional to bootstrap values). The branch lengths are proportional to the amount of evolutionary change, and the scale bars indicate substitutions per site.

Finally, we attempted to gain insight into the evolutionary trajectory of phenazine genes by contrasting the phylogeny of concatenated sequences of PhzA/B, PhzE, and PhzG proteins to that of the core *Burkholderia* genome estimated by using seven conserved housekeeping genes. This analysis produced phylogenetic trees with mostly congruent topologies (Fig. 2). One notable exception was discovered in strains *B. ubonensis* MSMB2058 and *B. ubonensis* MSMB2035, which are members of the Bcc group but harbor phenazine biosynthesis genes that are close to those from *B. singularis* TSV85, which belongs to the *B. pseudomallei* clade. The core phenazine genes of BGR1 and LMG 2196 clustered tightly within the Bcc clade, although both strains are members of the distinct *B. glumae/B. gladioli* clade.

We compared the overall organization and diversity of the phenazine pathways in *Burkholderia* spp. A comparison of genome sequences revealed the presence of three distinct types of phenazine cluster (Fig. 3 and Table S3). The first type is represented by a nine-gene operon found in *B. lata* ATCC 17760, most strains of the Bcc group, and *B. glumae*. In the second type, discovered in strains BDU5 and BDU6, the DNA segment carrying the *phzC* and *pcm3* genes is flipped. The third type of phenazine locus was identified in *B. ubonensis* strains MSMB2058 and MSMB2035 and in *B. singularis* TSV85. These strains shared an 18-gene phenazine cluster that was much larger than its counterparts in other *Burkholderia* and closely resembled genes involved in the synthesis of the phenazine esmeraldin from *Streptomyces antibioticus* (49). Interestingly, in *B. ubonensis* MSMB2035, the phenazine locus is located on a conjugative plasmid, pMSMB2035 (GenBank accession number NZ_CP013415), that forms part of this strain's genome. The analysis of the *Paraburkholderia* group identified only one species carrying phenazine genes, *P. phenazinium*. The chromosome-located *phz* cluster of this species is distinct from its counterparts in genomes of other *Burkholderia* spp. Finally, we also compared the genome regions flanking the phenazine genes in different strains of *Burkholderia*. This analysis revealed that in members of the Bcc group, the *phz* clusters are highly conserved but embedded in different spots of the genome, often adjacent to mobile genetic elements (Fig. S2).

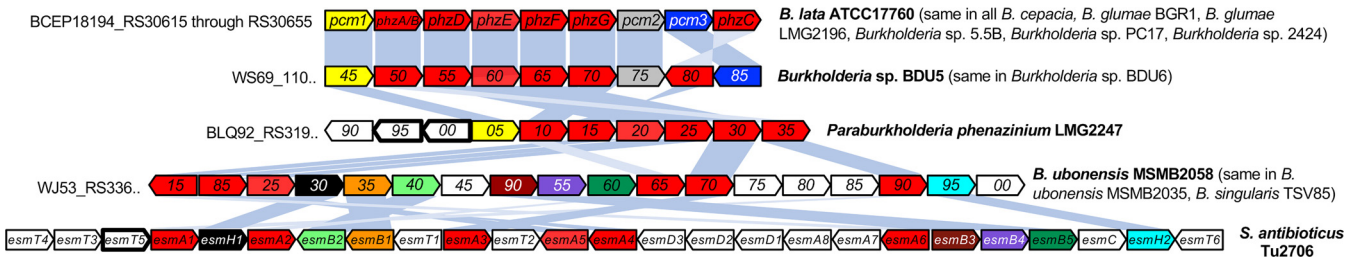

FIG 3 Gene organization of phenazine gene clusters in different species of *Burkholderia*. Comparison of the phenazine gene cluster of *B. lata* ATCC 17760 to its counterparts from other *Burkholderia* and *P. phenazinium* and to the esmeraldin biosynthesis (*esm*) locus of *Streptomyces antibioticus* Tu2706. Core biosynthesis genes are highlighted in red. Homologous modifying genes are indicated by arrows of the same color and connected with shading, whereas unique species-specific genes are shown by open arrows. The arrows with bold outlines indicate known or putative phenazine transport genes. The sizes of genes and intergenic regions are not to scale. Locus tags are shown using a code (e.g., the locus tag for the *pcm1* homolog of *Burkholderia* sp. BDU5 is WS69_11045). The predicted gene functions are summarized in Table S3.

Genetic analysis of phenazine biosynthesis in *B. lata* ATCC 17760. Our study was initiated by analyzing the spectrum of metabolites produced in strains carrying the full complement of phenazine biosynthesis genes of *B. lata*. The analysis of fractionated organic solvent extracts from the wild-type strain *B. lata* ATCC 17760, its complemented mutant *B. lata* phzA(pBBR1MCS-all), and *Pseudomonas synxantha* 2-79Z carrying a complete set of *phz* genes on the plasmid pUCP26-all identified dimethyl 4,9-dihydroxy-1,6-phenazinedicarboxylate as the final product of the pathway and revealed the presence of multiple phenazine intermediates (Fig. 4). The synthesis of phenazines in *B. lata* was strongly affected by the growth conditions, and best yields were observed in cultures grown in King's medium B (50). The levels of different phenazine derivatives were very dynamic (especially in the overproducer *B. lata* phzA (pBBR1-MCS-all) and may reflect an inherent feature of the regulation of *phz* genes in *Burkholderia* spp. All identified phenazine derivatives had close high-performance liquid chromatography (HPLC) retention times, eluting between 7 and 12 min under the applied conditions. Several phenazine compounds were detected (Fig. 4), three of which (2, 5, and 7) were purified and characterized in detail by nuclear magnetic resonance (NMR) (Fig. S4 to S12). Two other phenazine compounds (3 and 8) could not be isolated in sufficient quantities and were identified based on their HPLC-UV-mass spectrometry (MS) profiles. In addition, the UV analysis of other small peaks in the chromatogram indicated the presence of further phenazine derivatives. The analysis also identified three nonphenazine compounds, 9, 10, and 11. These dipeptides were produced by the wild-type *B. lata* but were absent from its phenazine-deficient mutants *phzA* and *pcm1*. The HPLC-MS analysis of isogenic mutants of *B. lata* revealed that the interruption of *phzA*, *pcm1*, and *pcm3* genes abolishes the production of all phenazines, which coincides with the loss of purple pigmentation (Fig. 5 and Fig. S13). The probing of *P. synxantha* 2-79Z carrying plasmids with different combinations of *phz* genes from ATCC 17760 correlated the presence of *pcm1* and *pcm2* genes with modifications of phenazine-1,6-dicarboxylic acid, which is the product of the core part of the pathway in *B. lata*. Specifically, *pcm2* was associated with the methylation of carboxyl moieties in positions 1 and 6, while *pcm1* was required for the hydroxylation of the phenazine ring at positions 4 and 9. Subsequent protein structure predictions with Phyre2 supported these observations and identified Pcm1 and Pcm2 as a flavin monooxygenase and an *S*-adenosylmethionine (SAM)-dependent methyltransferase, respectively. The product of the third putative modifying gene, *pcm3*, was identified as an NAD(P)H-dependent oxidoreductase, but its exact role in the conversion of PDC to dimethyl 4,9-dihydroxy-1,6-phenazinedicarboxylate remains unclear.

Biological function of phenazine compounds in *B. lata* ATCC 17760. The contribution of phenazines to the competitiveness and virulence of *Pseudomonas* has been documented in multiple studies. The opportunistic pathogen *P. aeruginosa* produces pyocyanin, which acts as a conserved virulence factor in mammals (30), invertebrates like *Drosophila melanogaster* (33) and *Caenorhabditis elegans* (32), and even plants (51).

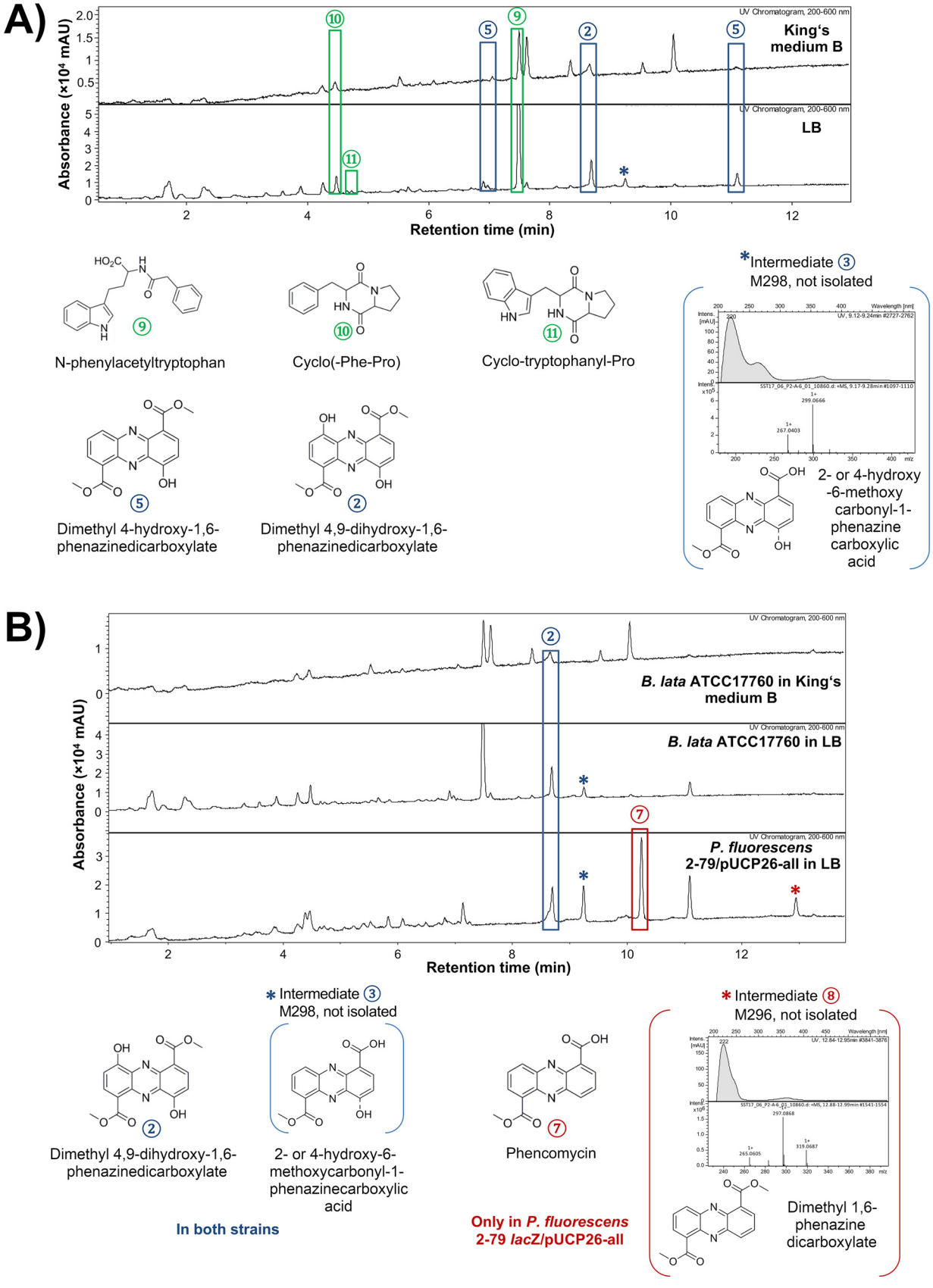

FIG 4 (A) Phenazine intermediates and other secondary metabolites identified in extracts of *B. lata* ATCC 17760 and (B) comparison of phenazines produced by *B. lata* and *P. synxantha* 2-79Z carrying the pUCP26-all plasmid. All phenazine derivatives are shown in blue, while the nonphenazine compounds are shown in green. Intermediates 3 and 8 could not be purified and were identified based on their HPLC-UV-MS profiles.

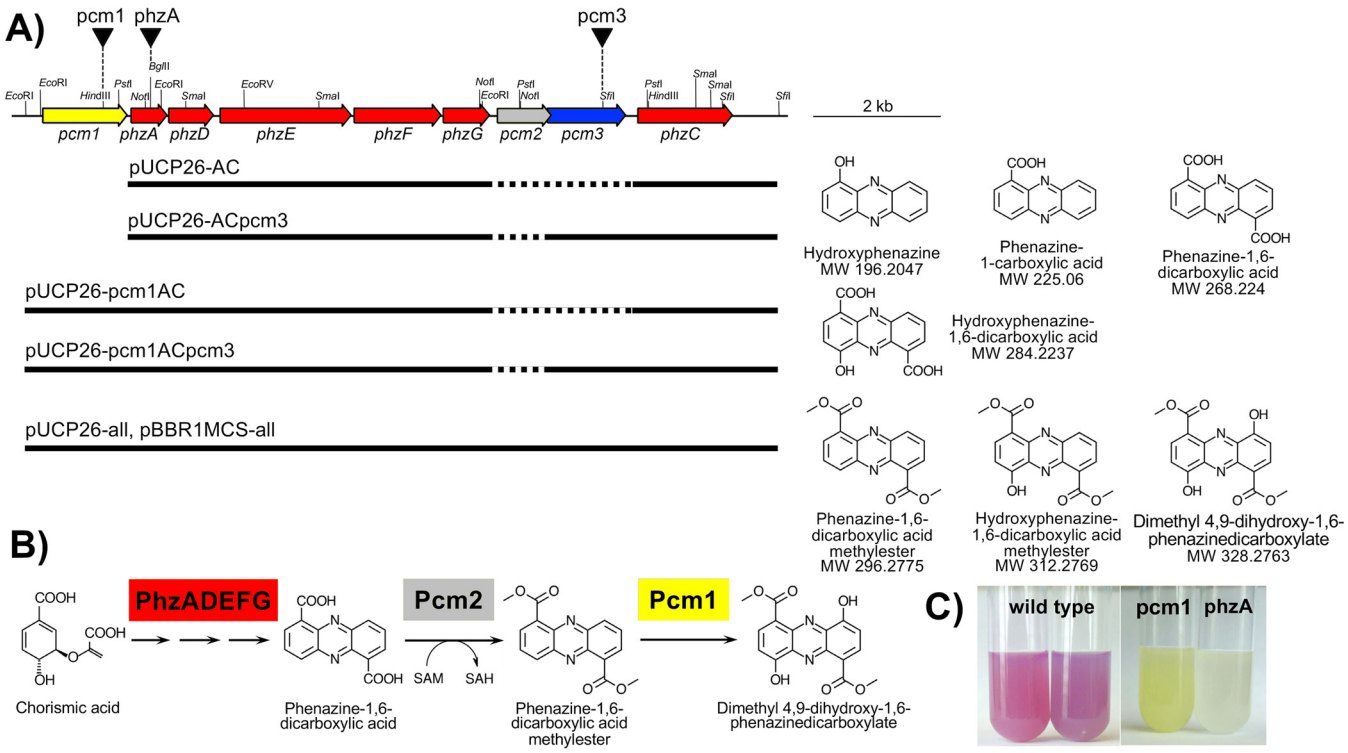

FIG 5 (A) Genetic organization of the phenazine biosynthesis cluster from *B. lata* ATCC 17760, isogenic mutants, and pUCP26-based plasmids containing different combinations of *phz* genes. Predicted genes are shown by colored arrows. DNA fragments cloned in plasmids under the control of *lac* promoter are indicated by thick lines. Inverted black triangles show insertions of the Tp^r cassette in the genome of *B. lata*. The right panel depicts structures of phenazines detected in *P. synxantha* 2-79Z carrying plasmids with *phz* genes by HPLC-coupled ESI-MS. (B) The proposed role of enzymes encoded by *pcm1* and *pcm2* in the biosynthesis of dimethyl 4,9-dihydroxy-1,6-phenazinedicarboxylate. (C) The appearance of wild-type *B. lata* ATCC 17760 and its *pcm1* and *phzA* mutants in King's medium B.

Members of the *Burkholderia cepacia* complex are opportunistic pathogens that are phenotypically similar to pseudomonads and occupy overlapping niches. Like *Pseudomonas*, they infect both vertebrate and invertebrate hosts, including nematodes (52) and fruit flies (53). Members of the Bcc complex are important postharvest plant pathogens associated with onion rot diseases (54). We hypothesized that phenazines might contribute to the virulence of *Burkholderia* and tested this hypothesis using the fruit fly infection assay of Castonguay-Vanier et al. (53) and the onion maceration assay of Jacobs et al. (54).

Results of these assays revealed that *Burkholderia* readily infects and kills *D. melanogaster* (51). With the exception of less-virulent *B. ambifaria*, all tested wild-type strains were lethal to flies and killed all inoculated animals within 40 h. In contrast, the survival of the control (10 mM $MgSO_4$) was over 86% (Fig. S3). In the second series of experiments, an attempt was made to slow the rate of killing by lowering the concentration of bacteria used to inoculate fruit flies. Since most *Burkholderia* species were highly virulent toward *D. melanogaster*, the concentration of inoculum was optimized in a dose-response experiment, where flies were inoculated with suspensions of *B. cepacia* ATCC 25416 and *B. lata* ATCC 17760 adjusted to 10^7, 10^6, and 10^5 CFU ml^{-1}. Results of these assays revealed that lower infection dose resulted in better survival of fruit flies, which at 10^5 CFU ml^{-1} approached 80%.

The third round of experiments compared the virulence toward fruit flies of the wild-type parental strain *B. lata* ATCC 17760, its isogenic mutants *phzA*, *pcm1*, and *pcm3*, and the phenazine-overproducing variant harboring the plasmid pBBR1MCS-all. The strains were applied at two inoculum levels: high (10^7 CFU ml^{-1}) and low (10^5 CFU ml^{-1}) (Table 1). The side-by-side comparison of ATCC 17760 and its phenazine-deficient and -overproducing derivatives showed no statistically significant difference between treatments at the lower inoculum level. At the higher inoculum level, the

TABLE 1 Fruit fly pathogenicity assays with *B. lata* ATCC 17760 and its isogenic phenazine mutant derivatives

	Inoculated at 10^7 CFU ml^{-1}		Inoculated at 10^5 CFU ml^{-1}	
Treatment[a]	% survival[a]	*P* value[b]	% survival[a]	*P* value[b]
B. lata ATCC 17760	3.3		76.7	
B. lata phzA	20.0	0.0232[c]	86.7	0.3193
B. lata pcm1	16.7	0.2639	86.7	0.4035
B. lata pcm3	20.0	0.0112[c]	73.3	0.1296
phzA (pBBR1MCS-all)	20.0	0.0227[c]	86.7	0.3144

[a]Percent survival after seven days.
[b]Pairwise comparison of each mutant and phenazine-overproducing derivative to the wild-type control strain using the two-sample survival log-rank test.
[c]The difference between this derivative and ATCC 17760 was significant. The experiment was repeated twice with similar results.

survivial of flies was significantly higher in the *phzA* and *pcm3* (but not *pcm1*) treatments. However, the phenazine-overproducing strain was less virulent than was the wild-type strain, thus suggesting against the involvement of phenazines in the virulence toward fruit flies.

We also tested four phenazine-producing and two nonproducing strains of *Burkhoderia* for their capacity to invade plant tissues and cause maceration of onion bulbs. The Phz$^-$ *B. cepacia* ATCC 25416 is a postharvest onion pathogen and was included as a positive control. Results of these assays separated the tested strains into two groups that exhibited, respectively, the high (ATCC 25416, PC39, PC17, 2424) and low (ATCC 17760 and AMMD) capacity to infect and damage onion bulbs (Table S1). However, as in the case of the fruit fly assays, no correlation was observed between the presence of phenazine biosynthesis genes and the degree of onion tissue maceration.

In fluorescent *Pseudomonas*, the formation of biofilms and their morphology are affected by the presence and nature of phenazine compounds. Many species of the *B. cepacia* complex are known for their capacity to form extensive biofilms, which prompted us to test the possible link between the synthesis of phenazines and formation of biofilms in *B. lata*. The biofilm assays compared the wild-type strain ATCC 17760, its phenazine-deficient *phzA* mutant, and the complemented mutant *B. lata* phzA(pBBR1MCS-all), which overproduces phenazines. The bacteria were inoculated in a flow cell connected to a BioFlux 200 microfluidic system and cultured in a medium conducive for the production of phenazines, King's medium B. The development of biofilms was monitored over 48 h by acquiring bright-field micrographs and subsequently analyzing them in the BioFlux Montage software. Results of these experiments revealed distinct differences in the dynamics of the establishment and development of biofilms in the three tested strains. In particular, the wild-type and overproducer strains attached faster and formed thicker biofilms than did the *phzA* mutant (Fig. 6). Interestingly, the phenazine-overproducing variant formed the densest biofilms that also did not dislodge in the medium flow, whereas mature biofilms of the wild-type strain readily dispersed. A similar trend was observed in static biofilm assays performed with the wild-type *B. lata* strain and its phenazine-deficient and complemented derivatives (Fig. 7). The crystal violet staining of biofilms formed in PVC plates revealed that ATCC 17760 and phzA(pBBR1MCS-all) bound significantly more dye ($P < 0.05$ by Kruskal-Wallis rank sum and Dunn's multiple comparison tests) than did the *phzA*, *pcm1*, and *pcm3* mutants. The most robust biofilm was observed in the complemented *phzA* mutant, thus mirroring the results obtained in the BioFlux flow cell system.

DISCUSSION

In this study, we attempted to comprehensively address the genetics, evolution, and biological role of phenazine compounds in *Burkholderia*. Although the production of phenazines in this economically important group of microorganisms was first

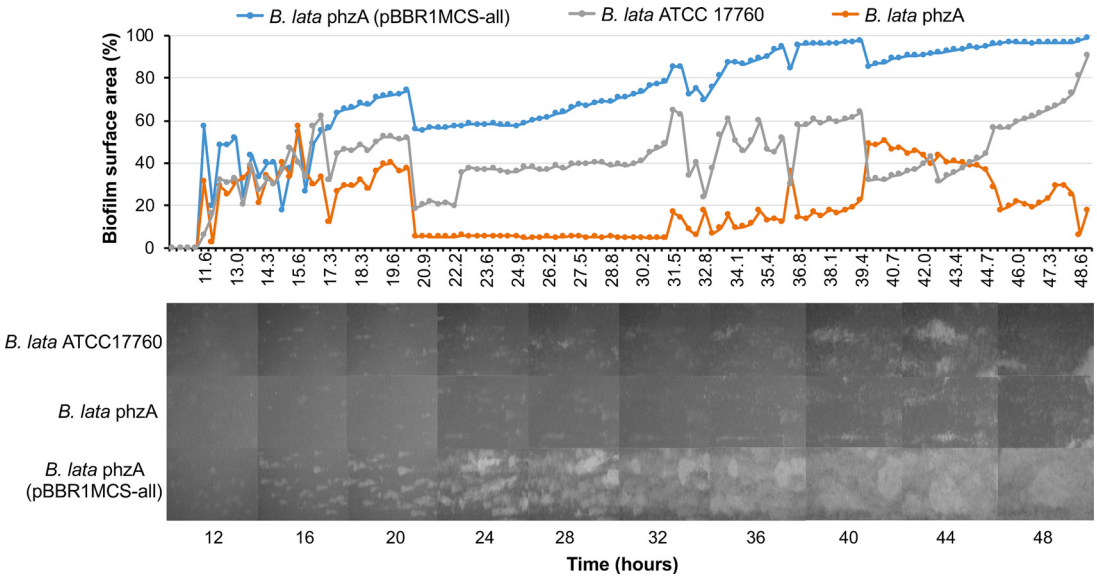

FIG 6 Comparison of flow cell biofilms formed by *B. lata* ATCC 17760, its phenazine-deficient mutant *B. lata* phzA and the phenazine-overproducing derivative *B. lata* phzA(pBBR1MCS-all). The three stains were inoculated into the BioFlux microfluidic system and allowed to form a biofilm for 48 h. The bright-field images were collected at 20 min intervals with an LS620 digital microscope. The top panel shows the percentage of surface area covered by the growing biofilm, whereas the bottom panel shows representative images of biofilm development over the course of the experiment.

reported almost 70 years ago (55), the access to recently generated genome sequences allowed us to assess the distribution, organization of biosynthesis gene clusters, and habitats that support this versatile and economically important group of phenazine-producing bacteria. Our results revealed that *phz* genes are present in genomes of many *Burkholderia* that have a worldwide origin and belong to different species of the genus. Most strains harboring *phz* genes were in the Bcc group and clustered closely with *B. cepacia*. We also identified phenazine clusters in some isolates of the *B. pseudomallei* clade, *B. lata* (ATCC 17760), *B. pyrrocinia* (strain 5.5B), and two strains of *B. ubonensis* (MSMB2035 and MSMB2058). Outside of the Bcc complex, we identified phenazine pathways in members of the *B. pseudomallei* group, including *B. singularis* TSV85

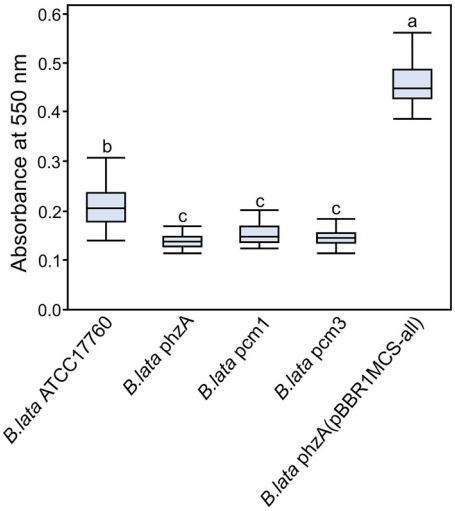

FIG 7 Static biofilms formed by *B. lata* ATCC 17760 and its phenazine-deficient and complemented derivatives. All strains were suspended in KMB broth at approximately 10^6 CFU ml^{-1} and grown in 96-well PVC plates for 48 h at 27°C, at which point the biofilms were stained with crystal violet. Treatments with different letters indicate significant differences as determined by the Kruskal-Wallis rank test followed by Dunn's multiple comparison test ($P < 0.05$).

TABLE 2 Bacterial strains, plasmids, and oligonucleotide primers used in this study

Strain, plasmid, or oligonucleotide primer	Relevant characteristics[a]	Reference or source
Bacteria		
Burkholderia lata ATCC 17760	Phz$^+$ wild type; soil isolate, Trinidad	46
Burkholderia lata phzA	Phz$^-$ mutant of ATCC 17760; *phzA*::*dhfrII*; Tp^r	This study
Burkholderia lata pcm1	Phz$^-$ mutant of ATCC 17760; *pcm1*::*dhfrII*; Tp^r	This study
Burkholderia lata pcm3	Phz$^-$ mutant of ATCC 17760; *pcm3*::*dhfrII*; Tp^r	This study
Burkholderia sp. 5.5B	Phz$^+$ wild type; soil isolate, USA	43
Burkholderia sp. 2424	Phz$^+$ wild type; uknown source, Japan	47
Burkholderia sp. PC17	Phz$^+$ wild-type strain; onion rhizosphere isolate, Japan	47
Burkholderia sp. PC39	Phz$^+$ wild-type strain; tobacco rhizosphere isolate, Japan	47
Burkholderia ambifaria AMMD	Phz$^-$ wild-type strain; rhizosphere isolate, USA	89
Burkholderia cepacia ATCC 25416	Phz$^-$ wild-type strain; onion isolate, USA	90
Pseudomonas synxantha 2-79	Phz$^+$ wild type; wheat rhizosphere isolate, USA	91
Pseudomonas synxantha 2-79Z	Phz$^-$ mutant of 2-79; *phzD*::*lacZ*; Rif^r	85
Escherichia coli S17-1(λ-pir)	*thi pro hsdM recA rpsL* RP4-2 (Tc^r::Mu) (Km^r::Tn*7*)	Lab collection
Escherichia coli DH5α	F$^-$ φ80*lac*ZΔM15 Δ(*lacZYA-argF*) U169 *recA1 endA1 hsdR17* (r_k^-, m_k^+) *gal*$^-$ *phoA supE44* λ^- *thi*-1 *gyrA96 relA1*	Invitrogen
Plasmids		
pBluescript II KS(+)	Cloning vector; Co1E1 f1(+) *lacZ*α *bla*; Ap^r	Stratagene
pUCP26	Broad-host-range vector; pMB1/pR01614 *lacZ*α *tet*; Tc^r	83
pBBR1MCS	Broad-host-range vector; pBBR1 *lacZ*α *mob cat*; Cm^r	84
p34S-Tp	Source of *dhfrII* cassette; ColE1 *bla aph*; Tp^r Ap^r	86
pEX18Tc	Gene replacement vector; pMB1 *mob sacB tet*	92
pUCP26-AC	pUCP26 with *phzADEFGC* genes of ATCC 17760	This study
pUCP26-ACpcm3	pUCP26 with *phzADEFGCpcm3* genes of ATCC 17760	This study
pUCP26-pcm1AC	pUCP26 with *pcm1phzADEFGC* genes of ATCC 17760	This study
pUCP26-pcm1ACpcm3	pUCP26 with *pcm1phzADEFGCpcm3* genes of ATCC 17760	This study
pUCP26-all	pUCP26 with the complete *phz* locus of ATCC 17760	This study
pBBR1MCS-all	pBBR1MCS with the complete *phz* locus of ATCC 17760	This study
Oligonucleotide primers		
pcm1f	5′-AATAGGTACCGTAAGTTTATTCTGGAGATGC-3′	This study
phzAf	5′-GAAATCAGGTACCTCGTGTAATCC-3′	This study
phzEf	5′-CCGCCATTCCTGATGCCGATAC-3′	This study
phzEr1	5′-GAAGATCCAGTACGCGCCGACC-3′	This study
phzEr2	5′-GTCCTGTAGGGATCCATAAAAAGCGTG-3′	This study
phzGf	5′-GCCTCACGAGATGGAATTCTGG-3′	This study
phzGr2	5′-TCCAATCGTTGCCATCGCGTTC-3′	This study
phzGr1	5′-ACAGACAGGATCCTTATCCGCAAG-3′	This study
pcm2f	5′-TTTTGGATCCAACCTTGATTCTCTTG-3′	This study
pcm3f	5′-TTTTGGATCCTTCGCCTCATCGAC-3′	This study
phzCf	5′-TAGCGGATCCGAGCGTGGGCGTC-3′	This study
phzCr	5′-TTTTTCTAGATGCGATTAGTTGTTGC-3′	This study
Tp-up	5′-ACGAACCCAGTTGACATAAG-3′	This study
Tp-low	5′-AGTGAGTTTTGTGCAATACC-3′	This study
Tet-up	5′-AGCGGTCCAGTGATCGAAGTTA-3′	This study
Tet-low	5′-CAGGAGTCGCATAAGGGAGAGC-3′	This study
SAC1	5′-GATGTTTTCTTGCCTTTGATGTTC-3′	93
SAC2	5′-GTCTTTGCATTAGCCGGAGATC-3′	93
Cm-up	5′-ATCCCAATGGCATCGTAAAGA-3′	87
Cm-low	5′-AAGCATTCTGCCGACAT-3′	87

[a]Phz, production of phenazine; Rif^r, rifampin resistance; Tp^r, trimethoprim resistance; Cm^r, chloramphenicol resistance; Km^r, kanamycin resistance; Tc^r, tetracycline resistance; *aph*, aminoglycoside 3′-phosphotransferase; *aacC1*, gentamicin acetyltransferase 3-1; *bla*, β-lactamase; *dhfrII*, dihydrofolate reductase. Underlined oligonucleotide bases represent restriction sites used in the cloning of amplicons as detailed in Materials and Methods.

and two strains, BDU5 and BDU6, that did not align closely with type strains and may represent new species of this clade. Finally, we confirmed the presence of *phz* genes in genomes of *B. glumae*.

Most of the presumed phenazine producers studied in this work were isolated from soil or diseased plants. Although listed as saprophytes, many strains of *Burkholderia* were closely related to species that are known to include numerous genetically close environmental and clinical isolates. Furthermore, several strains with *phz* genes belonged to *B.*

pseudomallei, a group that encompass serious pathogens of humans and animals (3). Interestingly, phenazine cluster seems to be commonly present in *B. glumae* since a study of strains native to the southern United States identified several virulent isolates that produced different pigments, one of which was later identified as the phenazine phencomycin (42, 56). Therefore, the question of the association of phenazine genes with the saprophytic and parasitic lifestyles of *Burkholderia* spp. clearly deserves further investigation.

While conducting this study, we were surprised to discover that the majority of presumed phenazine-producing *Burkholderia* were isolated in Australia. It is plausible that this prevalence simply reflects a nonrandom sampling, since similar strains were previously isolated in the United States (43, 56), Japan (47), Europe (23), and other parts of the world (46). Alternatively, it is possible that such strains are more common in specific locations, similar to some groups of phenazine-producing pseudomonads that are enriched in arid soils of the U.S. Pacific Northwest (57, 58) and *Fusarium* wilt-suppressive soils of Chateaurenard, France (59). It is tempting to speculate that a combination of particular environmental and edaphic factors may result in the enrichment of *Burkholderia* bacteria carrying *phz* genes in certain parts of the world, although further research is needed to test this hypothesis.

Our study revealed at least three distinct variants of phenazine clusters in *Burkholderia*. Most species of the *B. cepacia* and *B. glumae* clades shared an operon comprised of six core and three modifying biosynthesis genes. A variation of this scheme was observed in strains BDU5 and BDU6, which had a gene cluster with an inverted DNA segment containing the *phzC* and *pcm3* genes. Very different phenazine pathways were identified in *B. singularis* TSV85, *B. ubonensis* MSMB2035, and *B. ubonensis* MSMB2058. The *phz* clusters in these species had 18 genes, some of which encoded modifying enzymes similar to those involved in the synthesis of esmeraldin in *S. antibioticus* (49). Another distinct phenazine cluster was discovered in *P. phenazinium*, which differed from its *Burkholderia* counterparts in the number of core and modifying genes. Overall, these pathways differed in the number and types of predicted phenazine-modifying and efflux genes. All *Burkholderia* contained a full complement of core biosynthesis genes, although their arrangement and even structure varied among species. In particular, genomes of TSV85, MSMB2035, and MSMB2058 encoded a *Pseudomonas*-like version of PhzF that lacked the 120-amino acid N-terminal domain found in homologous proteins of other *Burkholderia* spp. These strains also carried an unusually long version of the isochorismatase PhzD, which represents a fusion of the *S*-adenosylmethionine-dependent methyltransferase and isochorismate hydrolase domains. Finally, the *phz* clusters of TSV85, MSMB2035, and MSMB2058 lacked the *phzC* gene but at the same time carried a gene encoding a canonical 3-deoxy-7-phosphoheptulonate synthase. We hypothesize that this enzyme compensates for the lack of PhzC and aids in the synthesis of phenazines by providing metabolic precursors for the shikimic acid pathway. Our results also revealed the conservation of *phz* clusters in most species of the Bcc group, as well as evidence for horizontal gene transfer in *B. glumae* and strains TSV85, MSMB2035, and MSMB2058, which harbor phenazine genes on conjugative plasmids. Although structurally conserved, the phenazine operons of Bcc strains are located in different genomic regions, which is likely a result of genomic relocation. Collectively, these findings suggest that the phenazine biosynthetic pathway of *Burkholderia* resembles its counterpart from *Pseudomonas* (25, 60, 61) in that it has a complex evolutionary history, which likely includes horizontal gene transfers among several distantly related groups of producing organisms.

Our experiments with *B. lata* ATCC 17760 represent formal confirmation of the involvement of the *phz* cluster in the production of dimethyl 4,9-dihydroxy-1,6-phenazinedicarboxylate. The assays with plasmids carrying deletion variants of the *B. lata phz* cluster also provide experimental evidence for the role of the three *pcm* genes in the modification of the phenazine tricycle during the synthesis of dimethyl 4,9-dihydroxy-

1,6-phenazinedicarboxylate. Overall, our results agree with the findings of Korth et al. (22) and indicate that the production of phenazine in Bcc strains is a highly dynamic process. The presence of multiple intermediates probably reflects the symmetrical nature of the final phenazine product, which is assembled via sequential hydroxylation and methylation of the PDC precursor. The dynamic nature and yield of different phenazine derivatives suggest the complex effects of the environment and of specific and global regulation, details of which remain entirely unknown.

Earlier studies reported the broad antibiotic activity of phenazines produced by several species of the genus *Burkholderia* (23, 42, 43). However, recent studies in *P. aeruginosa* prompted us to probe the biological role of phenazines in this diverse group of bacteria. Although we could not correlate the production of phenazines with the capacity of *Burkholderia* to kill fruit flies and rot onions, other experiments revealed a link between the presence and amount of phenazines and the dynamics of biofilm growth in both the flow cell and static experimental systems. These preliminary findings suggest that *Burkholderia*, like fluorescent pseudomonads, may benefit from the unique redox-cycling properties of phenazines and their capacity to act as extracellular electron shuttles in biofilms (62). These findings also suggest that the contribution of phenazines to the pathogenicity of members of the Bcc group should be revisited using chronic models of infection that often involve the biofilm mode of growth.

MATERIALS AND METHODS

Bacterial strains and plasmids. All strains and plasmids used in this study are listed in Table 2. Unless noted otherwise, *Burkholderia* and *Pseudomonas* were cultured at 27°C in Difco tryptic soy broth (TSB) (Becton, Dickinson, Franklin Lakes, NJ) or King's medium B (KMB) (50), while *Escherichia coli* cells were grown at 37°C in Luria-Bertani (LB) medium (63). Antibiotics were supplemented at the following concentrations: 100 μg ml^{-1} ampicillin (Ap), 30 or 100 μg ml^{-1} chloramphenicol (Cm), 100 μg ml^{-1} rifampin (Rif), 20 μg ml^{-1} tetracycline (Tc), and 10 or 50 μg ml^{-1} trimethoprim (Tp).

Bioinformatic techniques. Genome sequences of *Burkholderia* used in this study were acquired from several sources. Implementation of blast searches was used to screen publicly available repositories of bacterial genomes such as the National Center for Biotechnology Information (NCBI) GenBank (64), the Joint Genome Institute (JGI) Integrated Microbial Genomes and Microbiomes database (IGM/M) (65), and the *Burkholderia* Genome Database (66). Screening was accomplished by searching translated nucleotide databases with a protein query using the tblastn algorithm of BLAST v2.10.1 (67) and a cutoff E value of $<$1e$-$5. It has previously been described that in phenazine-producing bacteria, a small dimeric protein, PhzA/B, catalyzes the symmetrical condensation of two precursor molecules and is critical for the formation of the tricyclic phenazine ring (68). The amino acid sequence of PhzA/B from *B. lata* ATCC 17760 was used as a query for searching databases and identifying *Burkholderia* genomes that harbor phenazine loci. Analysis of the diversity and arrangement of the core, modifying, and auxiliary genes in *phz* clusters of *Burkholderia* spp. was conducted in Geneious 10.2.3 (Biomatters, Auckland, New Zealand) using reciprocal BLAST searches and the dotplot sequence comparisons with the European Molecular Biology Open Software Suite (EMBOSS) dotmatcher (69). The composition, physical properties, and possible cellular localization of proteins were identified using tools implemented in EMBOSS. Functional motifs were searched using regular expressions, generalized profiles, and hidden Markov models implemented in the MyHits database (http://myhits.isb-sib.ch/), and protein folds were predicted using the Phyre2 server (70). Flanking regions of phenazine loci were analyzed using the DNA G+C content. Sequences were screened using ISfinder (71) and Island Viewer (72) to identify genomic islands and genes encoding tRNAs, site-specific recombinases, and transposases. Phenazine gene clusters and flanking genomic regions were aligned with MAFFT v7.309 (73). The evolution of the *phz* pathway in *Burkholderia* was analyzed by establishing phylogenies inferred from sequences of core phenazine biosynthesis and housekeeping genes. Sequences were concatenated and aligned with MUSCLE (74), and phylogenetic trees were inferred with Geneious Tree Builder using the neighbor-joining (NJ) algorithm. The DNA and protein distances were corrected, respectively, by Kimura's two-parameter (75) and Jukes-Cantor (76) models of evolution. Final phylogenetic trees were visualized in iTOL (77). The pangenome analysis was performed using the Compute Pangenome app implemented in KBase (78).

In addition to publicly available genomes, genomes of strains *Burkholderia* sp. 5.5B, 2424, and PC17 also were sequenced, annotated, and used in bioinformatics analyses. The genomes were sequenced using a MiSeq instrument (Illumina, San Diego, CA) by the AgriLife Genomics and Bioinformatics Service at Texas A&M University (College Station, TX). The 150-bp paired-end reads were processed with Trimmomatic (79), assessed for quality with FastQC (https://www.bioinformatics.babraham.ac.uk/projects/fastqc/), and assembled with SPAdes v3.13.0 (80). The resultant assemblies were annotated with RASTtk (81) implemented in the Pathosystems Resource Integration Center (PATRIC) (82). Scaffolds of the final assemblies that contained phenazine biosynthesis genes were extracted from genome sequences and trimmed using Geneious v10.2.3.

Genetic analysis of phenazine biosynthesis genes. Plasmids carrying different combinations of *phz* genes from *B. lata* ATCC 17760 were used to identify phenazine products when certain biosynthetic

genes were inactive or deleted. The plasmids were generated by amplifying sets of *phz* genes by using PCR with primer sets listed in Table 2 and high-fidelity KOD Hot Start DNA polymerase (Millipore Sigma, Burlington, MA) and assembling them in the cloning vector pBluescript II KS(+). To assemble the phzAC fragment, three amplicons were generated with primer sets phzCf/phzCr, phzGr1/phzEf, and phzEr/phzAf and sequentially cloned in pBluescript II KS(+). The pcm1AC fragment was generated through the sequential cloning of amplicons generated with primer sets phzCf/phzCr, phzGr1/phzEf, and phzEr1/pcm1f, whereas the ACpcm3 gene set was assembled from fragments amplified with primers phzCr/pcm3f, phzGr1/phzEf, and phzEr1/phzAf. Similarly, the pcm1ACpcm3 segment was assembled by fusing the amplicons generated with primers phzCr/pcm3f, phzGr1/phzEf, and phzEr1/pcm1f. Finally, the complete phenazine pathway of ATCC 17760 was assembled from amplicons generated with primer sets phzCr/phzGf, phzGr2/phzEf, and phzEr1/pcm1f. The cloned gene sets were single-pass sequenced to ensure the absence of unwanted mutations, excised with XbaI and KpnI, and transferred into broad-host-range plasmid vectors pUCP26 (83) or pBBR1MCS (84) under the control of the *lac* promoter. The pUCP26-based plasmids were introduced for heterologous expression into the phenazine-deficient mutant strain *P. synxantha* 2-79Z (85), while the pBBR1MCS-based constructs were used in experiments with *B. lata* ATCC 17760.

To construct *pcm1* and *phzA* mutants of *B. lata* ATCC 17760, a 4,471-bp fragment of the *phz* locus was amplified using the high-fidelity KOD Hot Start DNA polymerase (Millipore Sigma) and primers pcm1f and phzEr2. The amplicon was digested with KpnI and BamHI and cloned into the gene replacement vector pEX18Tc, after which the *pcm1* and *phzA* genes were inactivated, respectively, by inserting the trimethoprim-resistance cassette from p34S-Tp (86) into unique HindIII and NotI sites. The *pcm3* mutant was constructed by amplifying a 3,439-bp fragment with primers pcm2f and phzCr, treating the amplicon with BamHI and XbaI, and cloning it into pEX18Tc. The resultant plasmid was further modified by inserting the Tp^r cassette into a unique SfiI site located within the *pcm3* gene. After verification by single-pass sequencing, all pEX18Tc-based plasmids were mobilized in *B. lata* from *E. coli* S17-1(λ-pir) and double crossover events were selected and verified by PCR with primer sets Tet-up/Tet-low and SAC1/SAC2 as described by Mavrodi et al. (87). Finally, the 2-79Z and ATCC 17760 derivatives harboring appropriate plasmids were generated by electroporation, selected by plating on LB agar supplemented with tetracycline or trimethoprim, and confirmed by PCR with plasmid-specific primers. All PCR amplifications, gene cloning, agarose gel electrophoresis, and electroporation were performed using standard techniques (63). Oligonucleotide primers were designed with Oligo v7.60 (Molecular Biology Insights, West Cascade, CO).

Identification of phenazine metabolites. Phenazine intermediates produced by plasmid-carrying derivatives and isogenic mutants were extracted and analyzed by HPLC-coupled mass spectrometry and NMR as follows. Bacteria were cultivated in LB medium at 30°C in shaking flasks at 160 rpm for 60 h (4 liters each). The pH was then adjusted to 2 with 20% (vol/vol) trifluoroacetic acid (TFA) before treatment in a Sonorex Digital 10P ultrasonic bath (Bandelin Electronic GmbH, Germany) for 15 min. Two percent (wt/vol) of Amberlite XAD16N absorber resin (Rohm & Haas GmbH, Germany) was added and the suspension was stirred for 3 h before removing the resin by filtration. The resin was then covered with 1.8 liters of ethyl acetate, stirred for 30 min, and left standing overnight. After removal of the resin, the remaining aqueous phase was separated, and the organic phase was dried with Na_2SO_4 before evaporation of the solvent in a rotary evaporator. The residual was dissolved in acetonitrile or methanol for further analysis.

Molecular masses were determined by mass spectrometry. Analysis involved separation of 2 μl sample on an Acquity-UPLC BEH C_{18} column (Waters GmbH, Germany) attached to a 1260 Infinity Series HPLC system (Agilent Technologies, Santa Clara, CA) and amaZon speed or maXis electrospray ionization (ESI)-based mass spectrometers (Bruker Daltonics GmbH, Germany) operated in the positive or negative mode. Chemical structures were determined by NMR spectroscopy. Toward this, sufficient amounts of the compounds were isolated by flash chromatography on a Reveleris X2 system (BÜCHI Labortechnik AG, Switzerland) equipped with a Reveleris C_{18}-RP cartridge (BÜCHI), followed by preparative HPLC (GX270 or PLC2250 system; Gilson Inc., USA) on C_{18}-RP columns (Kinetex C_{18} 100 Å or Gemini C_{18} 120 Å; Macherey-Nagel GmbH, Germany) developed in acetonitrile gradients. ^{1}H- and ^{13}C-NMR spectra were recorded on a 500 MHz Avance III (UltraShield Plus) spectrometer, equipped with a 5-mm RT BBO probe, or on a 700 MHz Avance III HD (Ascend) spectrometer, equipped with a 5-mm TCI cryoprobe (both from Bruker Biospin GmbH), at 298 K using acetone-d_6 or $CDCl_3$ as solvent (Fig. S4 to S12).

Pathogenicity assays. The contribution of phenazine metabolites to the virulence of *Burkholderia* was evaluated using the fruit fly (*Drosophila melanogaster*) infection assay of Castonguay-Vanier et al. (53). All bacterial cultures were grown in tryptic soy broth (TSB) to an optical density at 600 nm (OD_{600}) of 2. Cells were then washed with sterile 10 mM $MgSO_4$, suspended in the same buffer, and adjusted by serial dilution to the desired concentration. Ampicillin (500 mg ml^{-1}) was added to the cell suspensions to prevent possible infection with bacteria present on the surface of the fly. Adult flies of 8 ± 2 days were anesthetized with CO_2 and pricked in the dorsal thorax using a 27-gauge syringe needle previously dipped in the appropriate bacterial cell suspension. Control flies were pricked with a needle dipped into a solution of 10 mM $MgSO_4$ supplemented with ampicillin. The inoculated flies were maintained at 25°C and scored daily for survival. The infection assays were performed with a minimum of 30 flies for each strain, and all experiments were repeated in multiple repetitions. Differences between treatments were assessed using the two-sample survival log-rank test.

The ability of *Burkholderia* to infect onion bulbs was assessed according to Jacobs et al. (54). Onion bulbs were quartered using a sharp, sterile blade, and the quartered sections were separated into individual layers. Overnight cultures of *Burkholderia* spp. grown in TSB were adjusted to 10^7 CFU ml^{-1}, and 5-μl aliquots of bacterial suspensions were injected into onion slices using a sterile 10-μl pipette tip. The

inoculated slices were incubated at 27°C on water-saturated filter paper placed in petri plates. Tissue maceration was scored after 40 h on a scale of 0 to 3 (0, no visible maceration; 1, <33% maceration; 2, 34 to 65% maceration; 3, 66 to 100% maceration). *B. cepacia* ATCC 25416 is a known onion pathogen and was used as a positive control. The negative control was inoculated with 5 μl of TSB. The experiment was repeated twice with five replicates of each treatment, and differences between treatments were assessed according to the Fisher's protected least significant difference test ($P \leq 0.05$).

Biofilm assays. The effect of phenazines on biofilm formation was examined in *B. lata* ATCC 17760 and its phenazine-deficient isogenic mutant *B. lata* phzA and in an overproducing derivative carrying the pBBR1MCS-all plasmid. The ability to form static biofilms was determined using the crystal violet biofilm assay developed by O'Toole (88). Briefly, cultures were grown on LB plates supplemented with appropriate antibiotics for 24 h, bacteria were scraped off the agar, and the OD_{600} was adjusted to 0.1. The normalized suspensions were diluted 1:100 in KMB broth and 100 μl aliquots were dispensed into 96-well U-bottom Costar PVC microplates (Corning, Corning, NY). The inoculated microplates were incubated for 48 h at 27°C, after which all wells were gently rinsed with water to remove the unattached cells and media components. Crystal violet (0.1%) was added to each well, and after 15 min of staining the microplates were rinsed and dried and the retained dye was solubilized with 30% acetic acid and quantified by measuring absorbance at 550 nm. The experiments were repeated 4 times with 60 replicates per strain, and differences between treatments were assessed by Kruskal-Wallis rank test followed by Dunn's multiple comparison test ($P < 0.05$).

For flow cell biofilms, the bacteria were cultured overnight at 27°C on one-third-strength King's medium B (1/3 KMB) plates and then scraped off the surface of the agar and suspended in 1/3 KMB broth at a density of approximately 10^8 CFU ml^{-1}. The standardized bacterial suspensions were inoculated into a 24-well two inlets one outlet flow cell plate that was connected to a BioFlux 200 microfluidic system (Fluxion Biosciences, Alameda, CA). The inoculum was first pumped into the flow cell at 1.0 dyn/cm^2 for 6 sec, and bacteria were then allowed to attach to the channel surface for 1 h at 27°C. Initially, the flow rate of 0.16 dyn/cm^2 was maintained for the first 12 to 14 h, and after that, a flow rate of 0.44 dyn/cm^2 was set for 36 h to continuously pump fresh 1/3 KMB through channels containing bacteria. The development of biofilms was monitored by collecting bright-field images every 20 min with an LS620 digital microscope (Etaluma, Carlsbad, CA). The acquired images were merged into a time-lapse movie using BioFlux software (Fluxion). The images were also normalized using the threshold and slider tools of the BioFlux Montage software (Fluxion) and used to quantify the biofilm growth by calculating total percentage of area covered by the biofilm and plotting it against the time frames.

Data availability. The annotated genomes were deposited in the NCBI's GenBank under accession numbers JABUMO000000000, JABUMN000000000, and JABUMM000000000. The raw reads were deposited in the Sequence Read Archive (SRA) under accession numbers SRR11905455, SRR11905456, and SRR11905457. The genomes and SRA data were included in BioProject number PRJNA636525.

SUPPLEMENTAL MATERIAL

Supplemental material is available online only.

SUPPLEMENTAL FILE 1, PDF file, 2.9 MB.

SUPPLEMENTAL FILE 2, XLSX file, 8.3 MB.

SUPPLEMENTAL FILE 3, XLSX file, 0.01 MB.

ACKNOWLEDGMENTS

We thank Alex Flynt of the USM School of Biological, Environmental, and Earth Sciences for the help with fruit fly experiments. We also acknowledge the Mississippi INBRE, funded by an Institutional Development Award (IDeA) from the National Institute of General Medical Sciences of the National Institutes of Health under grant number P20GM103476.

REFERENCES

1. Woods SE, Sokol PA. 2006. The genus *Burkholderia*, p 848–860. *In* Dworkin M, Falkow S, Rosenberg E, Schleifer KH, Stackebrandt E (ed), The Prokaryotes, vol 5. Springer, New York.
2. Yabuuchi E, Kosako Y, Oyaizu H, Yano I, Hotta H, Hashimoto Y, Ezaki T, Arakawa M. 1992. Proposal of *Burkholderia* gen. nov. and transfer of seven species of the genus *Pseudomonas* homology group II to the new genus, with the type species *Burkholderia cepacia* (Palleroni and Holmes 1981) comb. nov. Microbiol Immunol 36:1251–1275. https://doi.org/10.1111/j.1348-0421.1992.tb02129.x.
3. Eberl L, Vandamme P. 2016. Members of the genus *Burkholderia*: good and bad guys. F1000Res 5:1007. https://doi.org/10.12688/f1000research.8221.1.
4. Estrada-de Los Santos P, Rojas-Rojas FU, Tapia-García EY, Vásquez-Murrieta MS, Hirsch AM. 2016. To split or not to split: an opinion on dividing the genus *Burkholderia*. Ann Microbiol 66:1303–1314. https://doi.org/10.1007/s13213-015-1183-1.
5. Sawana A, Adeolu M, Gupta RS. 2014. Molecular signatures and phylogenomic analysis of the genus *Burkholderia*: proposal for division of this genus into the emended genus *Burkholderia* containing pathogenic organisms and a new genus *Paraburkholderia* gen. nov. harboring environmental species. Front Genet 5:429. https://doi.org/10.3389/fgene.2014.00429.
6. Dobritsa AP, Samadpour M. 2016. Transfer of eleven species of the genus *Burkholderia* to the genus *Paraburkholderia* and proposal of *Caballeronia* gen. nov. to accommodate twelve species of the genera *Burkholderia* and *Paraburkholderia*. Int J Syst Evol Microbiol 66:2836–2846. https://doi.org/10.1099/ijsem.0.001065.
7. Wiersinga WJ, van der Poll T, White NJ, Day NP, Peacock SJ. 2006. Melioidosis: insights into the pathogenicity of *Burkholderia pseudomallei*. Nat Rev Microbiol 4:272–282. https://doi.org/10.1038/nrmicro1385.

8. Whitlock GC, Estes DM, Torres AG. 2007. Glanders: off to the races with *Burkholderia mallei*. FEMS Microbiol Lett 277:115–122. https://doi.org/10.1111/j.1574-6968.2007.00949.x.
9. Foong YC, Tan M, Bradbury RS. 2014. Melioidosis: a review. Rural Remote Health 14:2763.
10. Van Zandt KE, Greer MT, Gelhaus HC. 2013. Glanders: an overview of infection in humans. Orphanet J Rare Dis 8:131. https://doi.org/10.1186/1750-1172-8-131.
11. Sousa SA, Ramos CG, Leitao JH. 2011. *Burkholderia cepacia* complex: emerging multihost pathogens equipped with a wide range of virulence factors and determinants. Int J Microbiol 2011:1–9. https://doi.org/10.1155/2011/607575.
12. Stopnisek N, Zuhlke D, Carlier A, Barberan A, Fierer N, Becher D, Riedel K, Eberl L, Weisskopf L. 2016. Molecular mechanisms underlying the close association between soil *Burkholderia* and fungi. ISME J 10:253–264. https://doi.org/10.1038/ismej.2015.73.
13. Mahenthiralingam E, Urban TA, Goldberg JB. 2005. The multifarious, multireplicon *Burkholderia cepacia* complex. Nat Rev Microbiol 3:144–156. https://doi.org/10.1038/nrmicro1085.
14. Sawasdidoln C, Taweechaisupapong S, Sermswan RW, Tattawasart U, Tungpradabkul S, Wongratanacheewin S. 2010. Growing *Burkholderia pseudomallei* in biofilm stimulating conditions significantly induces antimicrobial resistance. PLoS One 5:e9196. https://doi.org/10.1371/journal.pone.0009196.
15. Lewis ER, Torres AG. 2016. The art of persistence-the secrets to *Burkholderia* chronic infections. Pathog Dis 74:ftw070. https://doi.org/10.1093/femspd/ftw070.
16. Compant S, Nowak J, Coenye T, Clement C, Ait Barka E. 2008. Diversity and occurrence of *Burkholderia* spp. in the natural environment. FEMS Microbiol Rev 32:607–626. https://doi.org/10.1111/j.1574-6976.2008.00113.x.
17. Stoyanova M, Pavlina I, Moncheva P, Bogatzevska N. 2007. Biodiversity and incidence of *Burkholderia* species. Biotechnol Biotechnol Eq 21:306–310. https://doi.org/10.1080/13102818.2007.10817465.
18. Keith LM, Sewake KT, Zee FT. 2005. Isolation and characterization of *Burkholderia gladioli* from orchids in Hawaii. Plant Dis 89:1273–1278. https://doi.org/10.1094/PD-89-1273.
19. Elshafie HS, Camele I, Racioppi R, Scrano L, Iacobellis NS, Bufo SA. 2012. *In vitro* antifungal activity of *Burkholderia gladioli* pv. *agaricicola* against some phytopathogenic fungi. Int J Mol Sci 13:16291–16302. https://doi.org/10.3390/ijms131216291.
20. Devescovi G, Bigirimana J, Degrassi G, Cabrio L, LiPuma JJ, Kim J, Hwang I, Venturi V. 2007. Involvement of a quorum-sensing-regulated lipase secreted by a clinical isolate of *Burkholderia glumae* in severe disease symptoms in rice. Appl Environ Microbiol 73:4950–4958. https://doi.org/10.1128/AEM.00105-07.
21. Martinucci M, Roscetto E, Iula VD, Votsi A, Catania MR, De Gregorio E. 2016. Accurate identification of members of the *Burkholderia cepacia* complex in cystic fibrosis sputum. Lett Appl Microbiol 62:221–229. https://doi.org/10.1111/lam.12537.
22. Korth H, Romer A, Budzikiewicz H, Pulverer G. 1978. 4,9-Dihydroxyphenazine-1,6-dicarboxylic acid dimethylester and the "missing link" in phenazine biosynthesis. J Gen Microbiol 104:299–303. https://doi.org/10.1099/00221287-104-2-299.
23. Smirnov V, Kiprianova E. 1990. Bacteria of Pseudomonas genus. Naukova Dumka, Kiev.
24. Guttenberger N, Blankenfeldt W, Breinbauer R. 2017. Recent developments in the isolation, biological function, biosynthesis, and synthesis of phenazine natural products. Bioorg Med Chem 25:6149–6166. https://doi.org/10.1016/j.bmc.2017.01.002.
25. Mavrodi DV, Peever TL, Mavrodi OV, Parejko JA, Raaijmakers JM, Lemanceau P, Mazurier S, Heide L, Blankenfeldt W, Weller DM, Thomashow LS. 2010. Diversity and evolution of the phenazine biosynthesis pathway. Appl Environ Microbiol 76:866–879. https://doi.org/10.1128/AEM.02009-09.
26. Shi YM, Brachmann AO, Westphalen MA, Neubacher N, Tobias NJ, Bode HB. 2019. Dual phenazine gene clusters enable diversification during biosynthesis. Nat Chem Biol 15:331–339. https://doi.org/10.1038/s41589-019-0246-1.
27. Dar D, Thomashow LS, Weller DM, Newman DK. 2020. Global landscape of phenazine biosynthesis and biodegradation reveals species-specific colonization patterns in agricultural soils and crop microbiomes. Elife 9:e59726. https://doi.org/10.7554/eLife.59726.
28. Chin-A-Woeng TFC, Bloemberg GV, Lugtenberg BJJ. 2003. Phenazines and their role in biocontrol by *Pseudomonas* bacteria. New Phytol 157:503–523. https://doi.org/10.1046/j.1469-8137.2003.00686.x.
29. Giddens SR, Houliston GJ, Mahanty HK. 2003. The influence of antibiotic production and pre-emptive colonization on the population dynamics of *Pantoea agglomerans* (*Erwinia herbicola*) Eh1087 and *Erwinia amylovora* in planta. Environ Microbiol 5:1016–1021. https://doi.org/10.1046/j.1462-2920.2003.00506.x.
30. Lau GW, Ran HM, Kong FS, Hassett DJ, Mavrodi D. 2004. *Pseudomonas aeruginosa* pyocyanin is critical for lung infection in mice. Infect Immun 72:4275–4278. https://doi.org/10.1128/IAI.72.7.4275-4278.2004.
31. Mavrodi DV, Blankenfeldt W, Thomashow LS. 2006. Phenazine compounds in fluorescent *Pseudomonas* spp.: biosynthesis and regulation. Annu Rev Phytopathol 44:417–445. https://doi.org/10.1146/annurev.phyto.44.013106.145710.
32. Mahajan-Miklos S, Tan MW, Rahme LG, Ausubel FM. 1999. Molecular mechanisms of bacterial virulence elucidated using a *Pseudomonas aeruginosa-Caenorhabditis elegans* pathogenesis model. Cell 96:47–56. https://doi.org/10.1016/S0092-8674(00)80958-7.
33. Lau GW, Goumnerov BC, Walendziewicz CL, Hewitson J, Xiao W, Mahajan-Miklos S, Tompkins RG, Perkins LA, Rahme LG. 2003. The *Drosophila melanogaster* Tol pathway participates in resistance to infection by the gram-negative human pathogen *Pseudomonas aeruginosa*. Infect Immun 71:4059–4066. https://doi.org/10.1128/iai.71.7.4059-4066.2003.
34. Cezairliyan B, Vinayavekhin N, Grenfell-Lee D, Yuen GJ, Saghatelian A, Ausubel FM. 2013. Identification of *Pseudomonas aeruginosa* phenazines that kill *Caenorhabditis elegans*. PLoS Pathog 9:e1003101. https://doi.org/10.1371/journal.ppat.1003101.
35. Dietrich LE, Teal TK, Price-Whelan A, Newman DK. 2008. Redox-active antibiotics control gene expression and community behavior in divergent bacteria. Science 321:1203–1206. https://doi.org/10.1126/science.1160619.
36. Okegbe C, Fields BL, Cole SJ, Beierschmitt C, Morgan CJ, Price-Whelan A, Stewart RC, Lee VT, Dietrich LEP. 2017. Electron-shuttling antibiotics structure bacterial communities by modulating cellular levels of c-di-GMP. Proc Natl Acad Sci U S A 114:E5236–E5245. https://doi.org/10.1073/pnas.1700264114.
37. Meisel JD, Panda O, Mahanti P, Schroeder FC, Kim DH. 2014. Chemosensation of bacterial secondary metabolites modulates neuroendocrine signaling and behavior of *C. elegans*. Cell 159:267–280. https://doi.org/10.1016/j.cell.2014.09.011.
38. Ciemniecki JA, Newman DK. 2020. The potential for redox-active metabolites to enhance or unlock anaerobic survival metabolisms in aerobes. J Bacteriol 202:e00797-19. https://doi.org/10.1128/JB.00797-19.
39. Bell SC, Turner JM. 1973. Iodinin biosynthesis by a pseudomonad. Biochem Soc Transact 1:751–753. https://doi.org/10.1042/bst0010751.
40. Morris MB, Roberts JB. 1959. A group of pseudomonads able to synthesize poly-beta-hydroxybutyric acid. Nature 183:1538–1539. https://doi.org/10.1038/1831538a0.
41. Ballard RW, Palleroni NJ, Doudoroff M, Stanier RY, Mandel M. 1970. Taxonomy of the aerobic pseudomonads: *Pseudomonas cepacia*, *P marginata*, *P alliicola* and *P caryophylli*. J Gen Microbiol 60:199–214. https://doi.org/10.1099/00221287-60-2-199.
42. Han JW, Kim JD, Lee JM, Ham JH, Lee D, Kim BS. 2014. Structural elucidation and antimicrobial activity of new phencomycin derivatives isolated from *Burkholderia glumae* strain 411gr-6. J Antibiot (Tokyo) 67:721–723. https://doi.org/10.1038/ja.2014.50.
43. Cartwright DK, Chilton WS, Benson DM. 1995. Pyrrolnitrin and phenazine production by *Pseudomonas cepacia*, strain 5.5B, a biocontrol agent of *Rhizoctonia solani*. Appl Microbiol Biotechnol 43:211–216. https://doi.org/10.1007/BF00172814.
44. Jeong Y, Kim J, Kim S, Kang Y, Nagamatsu T, Hwang I. 2003. Toxoflavin produced by *Burkholderia glumae* causing rice grain rot is responsible for inducing bacterial wilt in many field crops. Plant Dis 87:890–895. https://doi.org/10.1094/PDIS.2003.87.8.890.
45. Urakami T, Ito-Yoshida C, Araki H, Kijima T, Suzuki KI, Komagata K. 1994. Transfer of *Pseudomonas plantarii* and *Pseudomonas glumae* to *Burkholderia* as *Burkholderia* spp. and description of *Burkholderia vandii* sp. nov. Int J Syst Bacteriol 44:235–245. https://doi.org/10.1099/00207713-44-2-235.
46. Stanier RY, Palleroni NJ, Doudoroff M. 1966. The aerobic pseudomonads: a taxonomic study. J Gen Microbiol 43:159–271. https://doi.org/10.1099/00221287-43-2-159.
47. Seo ST, Tsuchiya K. 2004. PCR-based identification and characterization of *Burkholderia cepacia* complex bacteria from clinical and environmental sources. Lett Appl Microbiol 39:413–419. https://doi.org/10.1111/j.1472-765X.2004.01600.x.

48. Spilker T, Baldwin A, Bumford A, Dowson CG, Mahenthiralingam E, LiPuma JJ. 2009. Expanded multilocus sequence typing for *Burkholderia* species. J Clin Microbiol 47:2607–2610. https://doi.org/10.1128/JCM.00770-09.
49. Rui Z, Ye M, Wang S, Fujikawa K, Akerele B, Aung M, Floss HG, Zhang W, Yu TW. 2012. Insights into a divergent phenazine biosynthetic pathway governed by a plasmid-born esmeraldin gene cluster. Chem Biol 19:1116–1125. https://doi.org/10.1016/j.chembiol.2012.07.025.
50. King EO, Ward MK, Raney DE. 1954. Two simple media for the demonstration of pyocyanin and fluorescein. J Lab Clin Med 44:301–307.
51. Rahme LG, Ausubel FM, Cao H, Drenkard E, Goumnerov BC, Lau GW, Mahajan-Miklos S, Plotnikova J, Tan MW, Tsongalis J, Walendziewicz CL, Tompkins RG. 2000. Plants and animals share functionally common bacterial virulence factors. Proc Natl Acad Sci U S A 97:8815–8821. https://doi.org/10.1073/pnas.97.16.8815.
52. Wong YC, Abd El Ghany M, Ghazzali RNM, Yap SJ, Hoh CC, Pain A, Nathan S. 2018. Genetic determinants associated with in vivo survival of *Burkholderia cenocepacia* in the *Caenorhabditis elegans* model. Front Microbiol 9:1118. https://doi.org/10.3389/fmicb.2018.01118.
53. Castonguay-Vanier J, Vial L, Tremblay J, Deziel E. 2010. *Drosophila melanogaster* as a model host for the *Burkholderia cepacia* complex. PLoS One 5:e11467. https://doi.org/10.1371/journal.pone.0011467.
54. Jacobs JL, Fasi AC, Ramette A, Smith JJ, Hammerschmidt R, Sundin GW. 2008. Identification and onion pathogenicity of *Burkholderia cepacia* complex isolates from the onion rhizosphere and onion field soil. Appl Environ Microbiol 74:3121–3129. https://doi.org/10.1128/AEM.01941-07.
55. Turner JM, Messenger AJ. 1986. Occurrence, biochemistry and physiology of phenazine pigment production. Adv Microb Physiol 27:211–275. https://doi.org/10.1016/s0065-2911(08)60306-9.
56. Karki HS, Shrestha BK, Han JW, Groth DE, Barphagha IK, Rush MC, Melanson RA, Kim BS, Ham JH. 2012. Diversities in virulence, antifungal activity, pigmentation and DNA fingerprint among strains of *Burkholderia glumae*. PLoS One 7:e45376. https://doi.org/10.1371/journal.pone.0045376.
57. Mavrodi DV, Mavrodi OV, Parejko JA, Bonsall RF, Kwak YS, Paulitz TC, Thomashow LS, Weller DM. 2012. Accumulation of the antibiotic phenazine-1-carboxylic acid in the rhizosphere of dryland cereals. Appl Environ Microbiol 78:804–812. https://doi.org/10.1128/AEM.06784-11.
58. Parejko JA, Mavrodi DV, Mavrodi OV, Weller DM, Thomashow LS. 2012. Population structure and diversity of phenazine-1-carboxylic acid producing fluorescent *Pseudomonas* spp. from dryland cereal fields of central Washington state (USA). Microb Ecol 64:226–241. https://doi.org/10.1007/s00248-012-0015-0.
59. Mazurier S, Corberand T, Lemanceau P, Raaijmakers JM. 2009. Phenazine antibiotics produced by fluorescent pseudomonads contribute to natural soil suppressiveness to Fusarium wilt. ISME J 3:977–991. https://doi.org/10.1038/ismej.2009.33.
60. Fitzpatrick DA. 2009. Lines of evidence for horizontal gene transfer of a phenazine producing operon into multiple bacterial species. J Mol Evol 68:171–185. https://doi.org/10.1007/s00239-009-9198-5.
61. Biessy A, Novinscak A, Blom J, Leger G, Thomashow LS, Cazorla FM, Josic D, Filion M. 2019. Diversity of phytobeneficial traits revealed by whole-genome analysis of worldwide-isolated phenazine-producing *Pseudomonas* spp. Environ Microbiol 21:437–455. https://doi.org/10.1111/1462-2920.14476.
62. Glasser NR, Saunders SH, Newman DK. 2017. The colorful world of extracellular electron shuttles. Annu Rev Microbiol 71:731–751. https://doi.org/10.1146/annurev-micro-090816-093913.
63. Green MR, Sambrook J. 2012. Molecular cloning: a laboratory manual, 4th ed. Cold Spring Harbor Laboratory Press, Cold Spring Harbor, N.Y.
64. Benson DA, Clark K, Karsch-Mizrachi I, Lipman DJ, Ostell J, Sayers EW. 2014. GenBank. Nucleic Acids Res 42:D32–D37. https://doi.org/10.1093/nar/gkt1030.
65. Markowitz VM, Chen IM, Palaniappan K, Chu K, Szeto E, Grechkin Y, Ratner A, Jacob B, Huang J, Williams P, Huntemann M, Anderson I, Mavromatis K, Ivanova NN, Kyrpides NC. 2012. IMG: the integrated microbial genomes database and comparative analysis system. Nucleic Acids Res 40:D115–D122. https://doi.org/10.1093/nar/gkr1044.
66. Winsor GL, Khaira B, Van Rossum T, Lo R, Whiteside MD, Brinkman FS. 2008. The Burkholderia genome database: facilitating flexible queries and comparative analyses. Bioinformatics 24:2803–2804. https://doi.org/10.1093/bioinformatics/btn524.
67. Camacho C, Coulouris G, Avagyan V, Ma N, Papadopoulos J, Bealer K, Madden TL. 2009. BLAST+: architecture and applications. BMC Bioinformatics 10:421. https://doi.org/10.1186/1471-2105-10-421.
68. Blankenfeldt W, Parsons JF. 2014. The structural biology of phenazine biosynthesis. Curr Opin Struct Biol 29:26–33. https://doi.org/10.1016/j.sbi.2014.08.013.
69. Rice P, Longden I, Bleasby A. 2000. EMBOSS: the European molecular biology open software suite. Trends Genet 16:276–277. https://doi.org/10.1016/S0168-9525(00)02024-2.
70. Kelley LA, Mezulis S, Yates CM, Wass MN, Sternberg MJ. 2015. The Phyre2 web portal for protein modeling, prediction and analysis. Nat Protoc 10:845–858. https://doi.org/10.1038/nprot.2015.053.
71. Kichenaradja P, Siguier P, Perochon J, Chandler M. 2010. ISbrowser: an extension of ISfinder for visualizing insertion sequences in prokaryotic genomes. Nucleic Acids Res 38:D62–D68. https://doi.org/10.1093/nar/gkp947.
72. Dhillon BK, Laird MR, Shay JA, Winsor GL, Lo R, Nizam F, Pereira SK, Waglechner N, McArthur AG, Langille MG, Brinkman FS. 2015. IslandViewer 3: more flexible, interactive genomic island discovery, visualization and analysis. Nucleic Acids Res 43:W104–W108. https://doi.org/10.1093/nar/gkv401.
73. Katoh K, Standley DM. 2013. MAFFT multiple sequence alignment software version 7: improvements in performance and usability. Mol Biol Evol 30:772–780. https://doi.org/10.1093/molbev/mst010.
74. Edgar RC. 2004. MUSCLE: multiple sequence alignment with high accuracy and high throughput. Nucleic Acids Res 32:1792–1797. https://doi.org/10.1093/nar/gkh340.
75. Kimura M. 1980. A simple method for estimating evolutionary rates of base substitutions through comparative studies of nucleotide sequences. J Mol Evol 16:111–120. https://doi.org/10.1007/BF01731581.
76. Jukes TH, Cantor CR. 1969. Evolution of protein molecules, p 121–132. *In* Munro HN (ed), Mammalian protein metabolism. Academic Press, New York, N.Y.
77. Letunic I, Bork P. 2016. Interactive tree of life (iTOL) v3: an online tool for the display and annotation of phylogenetic and other trees. Nucleic Acids Res 44:W242–W245. https://doi.org/10.1093/nar/gkw290.
78. Arkin AP, Cottingham RW, Henry CS, Harris NL, Stevens RL, Maslov S, Dehal P, Ware D, Perez F, Canon S, Sneddon MW, Henderson ML, Riehl WJ, Murphy-Olson D, Chan SY, Kamimura RT, Kumari S, Drake MM, Brettin TS, Glass EM, Chivian D, Gunter D, Weston DJ, Allen BH, Baumohl J, Best AA, Bowen B, Brenner SE, Bun CC, Chandonia JM, Chia JM, Colasanti R, Conrad N, Davis JJ, Davison BH, DeJongh M, Devoid S, Dietrich E, Dubchak I, Edirisinghe JN, Fang G, Faria JP, Frybarger PM, Gerlach W, Gerstein M, Greiner A, Gurtowski J, Haun HL, He F, Jain R, et al. 2018. KBase: the United States Department of Energy systems biology knowledgebase. Nat Biotechnol 36:566–569. https://doi.org/10.1038/nbt.4163.
79. Bolger AM, Lohse M, Usadel B. 2014. Trimmomatic: a flexible trimmer for Illumina sequence data. Bioinformatics 30:2114–2120. https://doi.org/10.1093/bioinformatics/btu170.
80. Bankevich A, Nurk S, Antipov D, Gurevich AA, Dvorkin M, Kulikov AS, Lesin VM, Nikolenko SI, Pham S, Prjibelski AD, Pyshkin AV, Sirotkin AV, Vyahhi N, Tesler G, Alekseyev MA, Pevzner PA. 2012. SPAdes: a new genome assembly algorithm and its applications to single-cell sequencing. J Comput Biol 19:455–477. https://doi.org/10.1089/cmb.2012.0021.
81. Brettin T, Davis JJ, Disz T, Edwards RA, Gerdes S, Olsen GJ, Olson R, Overbeek R, Parrello B, Pusch GD, Shukla M, Thomason JA, 3rd, Stevens R, Vonstein V, Wattam AR, Xia F. 2015. RASTtk: a modular and extensible implementation of the RAST algorithm for building custom annotation pipelines and annotating batches of genomes. Sci Rep 5:8365. https://doi.org/10.1038/srep08365.
82. Wattam AR, Abraham D, Dalay O, Disz TL, Driscoll T, Gabbard JL, Gillespie JJ, Gough R, Hix D, Kenyon R, Machi D, Mao C, Nordberg EK, Olson R, Overbeek R, Pusch GD, Shukla M, Schulman J, Stevens RL, Sullivan DE, Vonstein V, Warren A, Will R, Wilson MJ, Yoo HS, Zhang C, Zhang Y, Sobral BW. 2014. PATRIC, the bacterial bioinformatics database and analysis resource. Nucleic Acids Res 42:D581–D591. https://doi.org/10.1093/nar/gkt1099.
83. West SE, Schweizer HP, Dall C, Sample AK, Runyen-Janecky LJ. 1994. Construction of improved *Escherichia-Pseudomonas* shuttle vectors derived from pUC18/19 and sequence of the region required for their replication in *Pseudomonas aeruginosa*. Gene 148:81–86. https://doi.org/10.1016/0378-1119(94)90237-2.
84. Kovach ME, Phillips RW, Elzer PH, Roop RM, 2nd, Peterson KM. 1994. pBBR1MCS: a broad-host-range cloning vector. Biotechniques 16:800–802.
85. Khan SR, Mavrodi DV, Jog GJ, Suga H, Thomashow LS, Farrand SK. 2005. Activation of the *phz* operon of *Pseudomonas fluorescens* 2–79 requires the LuxR homolog PhzR, *N*-(3-OH-hexanoyl)-L-homoserine lactone

produced by the LuxI homolog PhzI, and a cis-acting *phz* box. J Bacteriol 187:6517–6527. https://doi.org/10.1128/JB.187.18.6517-6527.2005.
86. Dennis JJ, Zylstra GJ. 1998. Plasposons: modular self-cloning minitransposon derivatives for rapid genetic analysis of Gram-negative bacterial genomes. Appl Environ Microbiol 64:2710–2715. https://doi.org/10.1128/AEM.64.7.2710-2715.1998.
87. Mavrodi OV, Mavrodi DV, Weller DM, Thomashow LS. 2006. Role of *ptsP*, *orfT*, and *sss* recombinase genes in root colonization by *Pseudomonas fluorescens* Q8r1-96. Appl Environ Microbiol 72:7111–7122. https://doi.org/10.1128/AEM.01215-06.
88. O'Toole GA. 2011. Microtiter dish biofilm formation assay. J Vis Exp 2437. https://doi.org/10.3791/2437.
89. Coenye T, Vandamme P, Govan JR, LiPuma JJ. 2001. Taxonomy and identification of the *Burkholderia cepacia* complex. J Clin Microbiol 39:3427–3436. https://doi.org/10.1128/JCM.39.10.3427-3436.2001.
90. Mahenthiralingam E, Coenye T, Chung JW, Speert DP, Govan JR, Taylor P, Vandamme P. 2000. Diagnostically and experimentally useful panel of strains from the *Burkholderia cepacia* complex. J Clin Microbiol 38:910–913. https://doi.org/10.1128/JCM.38.2.910-913.2000.
91. Weller DM, Cook RJ. 1983. Suppression of take-all of wheat by seed treatments with fluorescent pseudomonads. Phytopathology 73:463–469. https://doi.org/10.1094/Phyto-73-463.
92. Hoang TT, Karkhoff-Schweizer RR, Kutchma AJ, Schweizer HP. 1998. A broad-host-range Flp-FRT recombination system for site-specific excision of chromosomally-located DNA sequences: application for isolation of unmarked *Pseudomonas aeruginosa* mutants. Gene 212:77–86.
93. Mavrodi DV, Bonsall RF, Delaney SM, Soule MJ, Phillips G, Thomashow LS. 2001. Functional analysis of genes for biosynthesis of pyocyanin and phenazine-1-carboxamide from *Pseudomonas aeruginosa* PAO1. J Bacteriol 183:6454–6465. https://doi.org/10.1128/JB.183.21.6454-6465.2001.